

# Effect of Microstructure on Stress Corrosion Cracking of Alloy 600 and Alloy 690 in Caustic Solution

Kim Hong Pyo<sup>1)</sup>, Park Jung Kyu<sup>2)</sup>, Lim Yun Soo<sup>1)</sup> and Kim Joung Soo<sup>1)</sup>

1) Korea Atomic Energy Research Institute, Taejon, Korea

2) Dept. Metallurgical Engineering, ChungNam University, Taejon, Korea

## ABSTRACT

Stress corrosion cracking of Alloy 600 and Alloy 690 has been studied with a C-ring specimen in 10% and 40% NaOH at 315°C. SCC test was performed at 200mV above corrosion potential. Initial stress on the apex of C-ring specimen varied from 100 to 250% of yield strength. Solution annealed(SA) specimen was prepared by heat treatment at 1100°C for 30min followed by water quench. Sensitization treatment was performed at 600°C for 24 Hrs and thermal treatment(TT) at 715°C for 15Hrs. Sensitized Alloy 600 is more resistant to SCC compared to SA Alloy 600, suggesting that a beneficial effect of intergranular carbide prevail over harmful effect of Cr depletion around a grain boundary. Generally, SCC resistance of Alloy 600 increases in both 10% and 40% NaOH solution as the coverage of an intergranular carbide, defined as sum of an intergranular carbide length divided by grain boundary length, increases if the grain size of the Alloy 600s are almost same. Low temperature mill annealed Alloy 600 with small grain size and without intergranular carbide is most susceptible to SCC. SCC resistance of Ni- $\chi$ Cr-10Fe alloy also increases in both 10% and 40% NaOH solution as the Cr content of the alloy increases if the density of an intergranular carbide are almost same. So, TT Alloy 690 is most resistant to SCC. An empirical relationship of SCC rate with stress and NaOH concentration is developed.

## INTRODUCTION

Alloy 600 has been used as steam generator tubings in nuclear power plant because it has excellent corrosion resistance in primary and secondary coolant. But the Alloy 600 has undergone degradation such as intergranular attack and intergranular stress corrosion cracking(SCC) in the roll transition, U bend and tube to tube support plate intersection[1-3]. Failure analysis of pulled out tubes and results of hideout tests indicated that the caustic environment in the crevice was responsible for most of the intergranular attack and intergranular SCC of steam generator tubing materials[4].

Extensive research has been done to improve SCC resistance of steam generator tubings. High temperature mill annealed(HTMA) materials with intergranular carbide and large grain size showed better resistance to SCC than low temperature mill annealed(LTMA) materials with intragranular carbide and small grain size[5]. Thermal treatment(TT) producing semicontinuous intergranular carbide was reported to be beneficial to SCC resistance in primary water[6] and 10% NaOH[7]. Because SCC crack propagates along grain boundary, grain boundary chemistry has a critical influence on SCC resistance of Alloy 600 in caustic solution. Grain boundary chemistry can be viewed in terms of intergranular carbide distribution, Cr depletion around grain boundary and segregation of minor alloying element, C and impurities such as P, S and B into grain boundary. However relative contribution microstructural features to SCC is not clearly identified in caustic

environment.

LTMA Alloy 600, HTMA Alloy 600 and TT Alloy 600 are still used for steam generator tubing of many operating nuclear power plants. TT Alloy 690 is being used as a steam generator tubing of new and replaced steam generator of nuclear power plants. For life prediction and timely maintenance of nuclear power plant, it is very important to identify effect of environmental and mechanical parameter on SCC process.

The purpose of this work is to evaluate the effect of microstructure, stress and NaOH concentration on SCC in caustic solution

## EXPERIMENTAL PROCEDURE

Their chemical compositions are shown in Table 1. Four heats of HTMA Alloy 600s tubing, used in nuclear power plants, were provided by three tube manufacturers. Heat treatment of the HTMA Alloy 600A and TT Alloy 690 and their designation are shown in Table 2.

Table 1. Chemical Composition of Materials.

Material	Ni	Cr	Fe	C	S	P	B	N	Si	Cu	Al	Ti
HTMA Alloy 600 A	72.5	16.85	9.00	0.025	0.003	0.008	0.001	0.016	0.31	0.01	0.15	0.28
HTMA Alloy 600 B	74.76	15.63	8.62	0.025	<0.001	0.007	0.004	0.01	0.14	0.03	0.21	0.34
HTMA Alloy 600 C	76.11	15.29	7.57	0.026	0.001	0.008	0.004	0.004	0.15	0.015	0.23	0.32
HTMA Alloy 600 D	75.08	15.38	8.56	0.023	<0.001	0.006	0.003	0.01	0.20	<0.01	0.24	0.26
LTMA Alloy 600	75.34	15.97	8.03	0.04	0.001				0.30	0.11		
TT Alloy 600	58.9	29.57	10.54	0.02	0.001	0.009	0.0004	0.017	0.22	0.01	0.019	0.26

Carbide distribution of Alloy 600 was examined by electrolytic etching at 2.5~3V for 15~30sec in orthophosphoric acid and grain boundary being evaluated by electrolytic etching at 2.5~3V for 15~30sec in nital. Alloy 600 and Alloy 690 were also chemically etched in bromine for 15sec for carbide examination. A modified Huey test was carried out in boiling 25% $\text{HNO}_3$  for 48Hrs.

The 10% and 40% NaOH solutions were prepared by adding reagent grade NaOH to demineralized the water. Reference electrode and counter electrode were an external Ag/AgCl electrode and Pt wire, respectively. All the values of electrode potential were relative to that of external Ag/AgCl electrode unless otherwise indicated.

The SCC test was conducted in 10% and 40% NaOH using C-ring specimen at 315°C. The C-ring specimen was held at 200mV above corrosion potential. The stress at the apex of the C-ring specimen was varied from 150% to 250% of room temperature yield strength by changing outer diameter displacement of the C-ring. The SCC fracture surface and cross-sectional area of C-ring specimen were examined with both SEM and optical microscope.

Table 2. Heat Treatment and Designation of Alloy.

SA Alloy 600	solution annealed at 1100°C for 30min and then water quenched(SA)
SASEN Alloy 600	sensitized at 600°C for 24Hrs following SA
SATT Alloy 600	thermally treated at 715°C for 15Hrs following SA
HTMA Alloy 600	commercially high temperature mill annealed
HTMASEN Alloy 600	sensitized at 600°C for 24Hrs following HTMA
HTMATT Alloy 600	thermally treated at 715°C for 15Hrs following HTMA
SA Alloy 690	solution annealed at 1150°C for 30min and then water quenched
TT Alloy 690	thermally treated at 720°C for 10Hrs

## RESULTS AND DISCUSSION

### Microstructure

Four heats of HTMA Alloy 600s tubing have similar intergranular carbide distribution, Cr and C content, grain size and mechanical properties as shown in Table 3.

Table 3. Metallurgical Characteristics and Mechanical Properties of HTMA Alloy 600s.

Alloy	ASTM Grain Size No.	Intergranular Carbide Distribution	Yield Strength (ksi)	Tensile Strength (ksi)	Elongation(%)
HTMA Alloy 600A	5.0	discontinuous	41.4	98.8	43
HTMA Alloy 600B	5.0	discontinuous	35.5	94	46
HTMA Alloy 600C	6.0	discontinuous	37.1	97.1	44
HTMA Alloy 600D	5.5	discontinuous	37.7	95.5	43.5

HTMA Alloy 600 has abundant intragranular carbides and few intergranular carbides and has small grain size compared to that of HTMA Alloy 600. TT Alloy 690 has intergranular carbides. Intergranular carbide length and spacing between intergranular carbide vary from boundary to boundary and even in the boundary. Intergranular carbide length and spacing between intergranular carbides vary significantly for HTMA Alloy 600 in which some boundary has no intergranular carbides while the other boundary has small (about 1 $\mu$ m long) and closely spaced intergranular carbides. The boundary without intergranular carbides seems to be a low angle grain boundary or twin boundary. Average intergranular carbide length and coverage of intergranular carbide in grain boundary, defined as sum of intragranular carbide divided by grain boundary length are shown in Table 4. Intergranular carbide in HTMASEN Alloy 600 is relatively evenly distributed compared to that in

HTMA Alloy 600 and its average length and thickness are larger than those of HTMA. Intergranular carbide in HTMATT Alloy 600 is about 2 $\mu$ m and longer than that in HTMA SEN Alloy 600. Intergranular carbide spacing in HTMATT Alloy 600 is about 0.2 $\mu$ m and more closely spaced than that in HTMA SEN Alloy 600. All boundary except twin boundary has intergranular carbides. The extent of variation in intergranular carbide length and their spacing for HTMATT Alloy 600 is least among Alloy 600s used in this work. Intergranular carbide in TT Alloy 690 is about 0.45 $\mu$ m long and their spacing is about 0.02 $\mu$ m.

Table 4. Intergranular Carbide Length, Thickness and a Fraction of Intergranular Carbide in Grain Boundary.

Alloy	Intergranular Carbide Length( $\mu$ m)	Intergranular Carbide Thickness( $\mu$ m)	Coverage of Intergranular Carbide in Grain Boundary(%)
HTMA Alloy 600	0.28	0.15	28
HTMA SEN Alloy 600	0.41	0.20	80
HTMATT Alloy 600	0.57	0.29	89
TT Alloy 690	0.45	0.15	96

The degree of Cr depletion around grain boundary measured with Modified Huey test is shown in Table 5. Precipitation of intergranular carbide simultaneously produces Cr depletion around grain boundary. But the Cr depletion around grain boundary is healed by Cr diffusion from matrix back into the grain boundary if heat treatment temperature and time is high and long enough. SA Alloy 600 shows a very slight weight loss because it is cooled too fast from solution anneal temperature to room temperature to precipitate intergranular carbide. SA SEN Alloy 600 shows significant weight loss because of extensive precipitation of intergranular carbide and concurrent Cr depletion around grain boundary. SATT Alloy 600 shows much less weight loss compared to SA SEN Alloy 600 because heat treatment temperature is high enough for Cr diffusion from matrix back to the Cr depleted grain boundary. HTMA Alloy 600 shows greater weight loss than SA Alloy 600 because it has intergranular precipitate produced during cool down from mill anneal temperature to around 500°C. HTMA SEN Alloy 600 and HTMATT Alloy 600 are similar to SA SEN Alloy 600 and SATT Alloy 600 in weight loss, respectively because heat treatments are same after solution anneal or mill anneal.

### Stress Corrosion Cracking

The maximum SCC rate of SA Alloy 600, SA SEN Alloy 600 and SATT Alloy 600 tested in 40% NaOH at 315°C is shown in Table 6. SCC rate measured with CT specimen as a function of stress intensity factor showed two stages for SCC crack growth; stress intensity dependent slow SCC crack growth stage and almost stress independent fast SCC crack growth stage[8]. In this work we do not differentiate between the two stages because SCC crack length is not measured insitu. In addition, SCC crack initiation period is ignored in estimating the maximum SCC rate. Maximum SCC rate is estimated by dividing maximum SCC crack length with exposure time to the test environment. The maximum SCC rate decreases with a

following order : SA Alloy Alloy 600, SASEN Alloy 600 and SATT alloy 600. Grain size of SA Alloy 600, SASEN Alloy 600 and SATT alloy 600 are almost same because heat treatment at 600°C after mill anneal is not high enough for grain growth to occur. Maximum SCC rate of HTMA Alloy 600, HTMASEN Alloy 600 and HTMATT alloy 600 in 10% NaOH and 40% NaOH at 315°C is shown in Table 7. Maximum SCC rate decrease with a following order in 10% NaOH and 40% NaOH: HTMA Alloy 600, HTMASEN Alloy 600 and HTMATT alloy 600. Grain size of HTMA Alloy 600, HTMASEN Alloy 600 and HTMATT alloy 600 are almost same. Because SCC crack propagates along the grain boundary, grain boundary chemistry has critical influence on SCC resistance of Alloy 600 in caustic solution. Grain boundary chemistry can be viewed in terms of intergranular carbide distribution, Cr depletion around grain boundary and segregation of minor alloying element, C and impurities such as P, S and B into the grain boundary.

Table 5. Weight Loss Measured in Boiling HNO<sub>3</sub> for 48Hrs (Modified Huey test).

Alloy	SA Alloy 600	SASEN Alloy 600	SATT Alloy 600	HTMA Alloy 600	HTMASEN Alloy 600	HTMATT Alloy 600
Weight loss(kg/m <sup>2</sup> /sec)	20×10 <sup>-9</sup>	627×10 <sup>-9</sup>	18×10 <sup>-9</sup>	115×10 <sup>-9</sup>	*	22×10 <sup>-9</sup>

\*: completely disintegrated

Table 6 Maximum SCC Rate of SA Alloy 600, SASEN Alloy 600 and SATT Alloy 600 in 40% NaOH at 315°C and at a Initial Stress of 150% YS

Alloy	SA Alloy 600	SASEN Alloy 600	SATT Alloy 600
Maximum SCC Rate(m/sec)	4.8×10 <sup>-9</sup>	4.0×10 <sup>-9</sup>	0.7×10 <sup>-9</sup>

Table 7 Maximum SCC Rate of HTMA Alloy 600, HTMASEN Alloy 600 and HTMA TT Alloy 600 with a Initial Stress of 250% of YS in 10% and Those with a Initial Stress of 150% of YS in 40% NaOH at 315°C.

Alloy	HTMA Alloy 600	HTMA SEN Alloy 600	HTMA TT Alloy 600
Maximum SCC Rate(m/sec) in 10% NaOH	1.7×10 <sup>-9</sup>	1.3×10 <sup>-10</sup>	7.7×10 <sup>-10</sup>
Maximum SCC Rate(m/sec) in 40% NaOH	5.4×10 <sup>-9</sup>	3.1×10 <sup>-9</sup>	0.6×10 <sup>-9</sup>

Recent work performed with an atom probe found that C segregation in Alloy 600 for heat treatment at 600°C increases up to intergranular carbide precipitation and then decreases by precipitation of intergranular carbide with further heat treatment time[9]. A little P segregation is observed when excess carbon is less than 0.3nm<sup>2</sup>. B and N segregation to grain boundary is not related with heat treatment. So, segregation of minor alloying element, C and impurities such as S, P, B, N seems to have no effect on SCC of SASEN Alloy 600 and SATT Alloy 600 because heat treatment time employed in this

work is long enough to rule out effect of segregation on SCC.

The big difference of SA Alloy 600 and SATT Alloy 600 in grain boundary chemistry is the presence of intergranular carbide in SATT Alloy 600 since SA Alloy 600 has no intergranular carbide. So, higher resistance of SATT Alloy 600 than SA Alloy 600 can be attributed to the presence of intergranular carbide in SATT Alloy 600. SA Alloy 600 is more susceptible to SCC than SASEN Alloy 600. Our previous work found that the SCC rate of solution annealed Ni- $\chi$ Cr-10Fe alloy decreases with Cr content in 40% NaOH at 315°C[10]. So, Higher SCC resistance of SASEN Alloy 600 than SA Alloy 600 implies that beneficial effect of intergranular carbide prevails over harmful effects of Cr depletion in caustic solution. Higher SCC resistance of SATT Alloy 600 than SASEN Alloy 600 is partly due to presence of more closely spaced intergranular carbide and partly due to healing of Cr depletion around grain boundary in SATT Alloy 600. Relative SCC resistance of HTMA Alloy 600, HTMASSEN Alloy 600, HTMATT Alloy 600 also can be explained with a beneficial effect of intergranular carbide for SCC in 10% NaOH and 40% NaOH because a density of intergranular carbide in grain boundary, which is defined as sum of intergranular carbide length divided by grain boundary length, increases with a following order: HTMA Alloy 600, HTMASSEN Alloy 600 and HTMATT Alloy 600.

Maximum SCC rates of as received four HTMA Alloy 600s, an LTMA Alloy 600 and TT Alloy 690 tested in 10% NaOH at 315°C are shown in Fig. 1. SCC rates of four HTMA Alloy 600s are almost the same, presumably due to nearly equal intergranular carbide distribution and grain size even though the four HTMA Alloy 600s are provided by three tube manufacturers. LTMA Alloy 600 is extremely susceptible to SCC due to an absence of intergranular carbide and partly due to small grain size. Kim, et. al.[10] investigated SCC resistance of SA Alloy 600 with varying grain sizes in 40% NaOH at 315°C and found that SCC resistance increases with grain size. TT Alloy 690 is most resistant to SCC because the TT Alloy 690 has semi continuous intergranular carbide and high Cr content of about 30%, which is almost two times the Cr content of Alloy 600.

The maximum SCC rate of Alloy 600 with stress is shown in Fig. 2. Maximum average SCC rate rapidly increases in 10% NaOH and 40% NaOH as the initial applied stress at the apex of C-ring increases. The slope of log-log plot in Fig.6 is in the range from 0.14 to 4.44. HTMA Alloy 600 and TT Alloy 600 are relatively susceptible to SCC, therefore it seems to be that the HTMA Alloy 600 and the HTMASSEN Alloy 600 stressed to 250% of yield stress were already through wall cracked long before they are took out to examine SCC. So, the actual slopes in log-log plot of the HTMA Alloy 600 and the HTMASSEN Alloy 600 would be rather higher than those reported in this work. The slope of HAMATT Alloy 600, 4.44, in Fig. 6 is in relatively good agreement with that measured with constant load in pure H<sub>2</sub>O at 365°C even though test environments are quite different from each other. These results indicate that the SCC Alloy 600 in caustic as well as in pure H<sub>2</sub>O is highly dependent on stress.

Maximum SCC rate increases very dramatically with NaOH concentration as shown in Fig.3. Maximum SCC rate increases more than 2 order as NaOH concentration increases 4 times. Vailant, et. al.[11], suggested that SCC crack growth rate in slow crack growth stage is proportional to  $[\text{NaOH}]^b$ , where b is about 0.66 for MA Alloy 600 and about 1 for TT Alloy 600. But it is not clearly identified whether the SCC crack growth rate model is for SCC at free corrosion potential or at controlled potential. The SCC rate measured at 200mV above corrosion potential in caustic solution in this work suggests that b is about 2.4 if SCC crack growth rate follows the rate equation suggested by Vailant, et.al.. So, SCC rate,  $V$ , seems to be given by following equation in caustic solution:

$$V=A\sigma^{4.4}[\text{NaOH}]^{2.4} \quad (1)$$

Where  $\sigma$  is stress,  $[\text{NaOH}]$  is NaOH concentration in wt. % and A is constant. The above equation shows that SCC rate is highly dependent on stress and NaOH concentration in caustic solution.

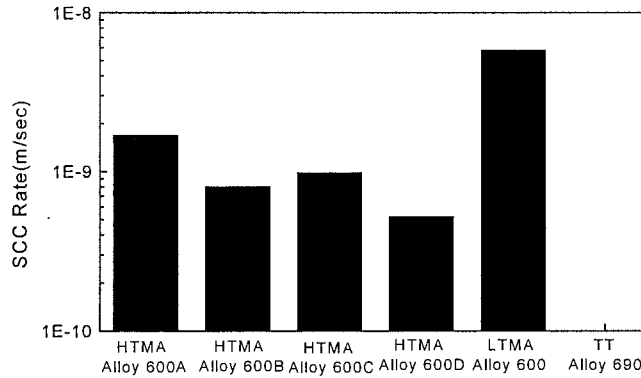


Fig.1 SCC Rate of Staem Generator Materials in 10% NaOH at 315°C

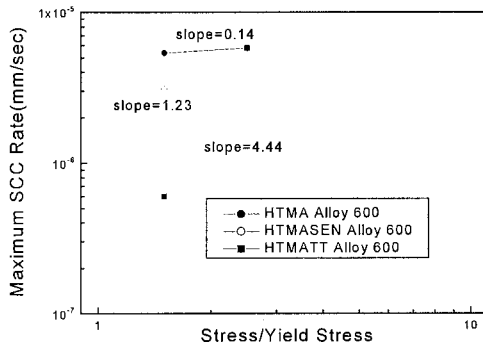


Fig.2 Stress dependency of SCC rate in 40% NaOH at 315°C

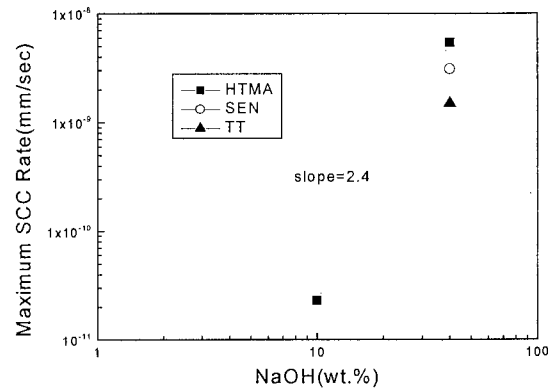


Fig.3 NaOH concentration dependency of SCC rate stressed at 150% YS and at 315°C

## CONCLUSION

SASEN Alloy 600 is more resistant to SCC compared to SA Alloy 600, suggesting that a beneficial effect of intergranular carbide will prevail over the harmful effects of Cr depletion around the grain boundary. Generally, SCC resistance of Alloy 600 increases in both 10% and 40% NaOH solution as the coverage of an intergranular carbide, defined as the sum of an intergranular carbide length divided by grain boundary length, increases if the grain size of the Alloy 600s are

almost the same. Low temperature mill annealed Alloy 600 with small grain size and without intergranular carbide is most susceptible to SCC. SCC resistance of Ni- $\gamma$ Cr-10Fe alloy also increases in both 10% and 40% NaOH solution as the Cr content of the alloy increases if the density of an intergranular carbide are almost comparable. So, TT Alloy 690 is most resistant to SCC. An empirical relationship of SCC crack growth rate,  $V$ , with stress,  $\sigma$  (ksi) and NaOH concentration in wt.%, [NaOH], is developed as  $V=A(\sigma)^{4.4} [\text{NaOH}]^{2.5}$ , where A is a constant.

## ACKNOWLEDGEMENT

This work has been done as a part of the Steam Generator Project of the Mid and Long-Term Program financially supported by the MOST in Korea.

## REFERENCES

1. Chae, S. G., Kim, U. C. and Kim, J.S. , *Failure Analysis of Pulled out tube from Kori 2*, KAERI, 1990.
2. Kim, U. C, Kim, J. S, Hwang, S. S, Jung, H. S., Kim, H. P. and Hur, D. H., *Failure Analysis of Pulled out tube from Kori 1*, KAERI, 1992.
3. Kim, U. C., Kim, J. S. and Kim, H. P., *Failure Analysis of Pulled out tube from Kori 1*, KAERI, 1995.
4. Lumsden, J. B., Jeanjaguet, S. L., Paine, J. P. N and Mcliree, A., "Mechanism and Effectiveness of Inhibitors for SCC in a Caustic Environment, *7th International Symposium on Environmental Degradation of Materials in Nuclear Power Systems- Water Reactors*, pp. 317-325, Breckenridge, Colorado, USA, August, 1995.
5. Crum , J. R. and . Nagashima, T., "Review of Alloy 690 Steam Generator Studies", *Proc. of the 8th Intern. Symp.on Environmental Degradation of Materials in Nuclear Power Systems- Water Reactors*, pp.127-137, Amelia Island, Fl, USA, 1997,.
6. Was, G. S. and Lian, K., "Role of Carbides in Stress Corrosion Cracking of Alloy 600 and Controlled Purity Ni-16%Cr 9%Fe in Primary Water at 360°C", *Met. Trans. A* Vol. 23A No.4 1992, pp. 675-688.
7. Airey, G. P. *Optimization of Metallurgical Variables to Improve the Stress Corrosion Resistance of Inconel 600*, EPRI NP-1354, March 1980.
8. Shen, C. H. and Shewmon, P. G., "A Mechanism for Hydrogen-Induced Intergranular Stress Corrosion Cracking in Alloy 600," *Met. Trans. A*, Vol.21A, 1990, pp. 1261-1271.
9. Thuvander, M., Miller, M. K. and Stiller, K., "Grain Boundary Segregation during Heat Treatment at 600°C in a Model Alloy 600," *Met. Sci. and Eng.*, Vol. A270, 1999, pp. 38-43
10. Kim, H.P., Hwang, S. K., Lim, Y. S., Kuk I. H. and Kim, J. S., to be published in *Metals and Materials*, 2001
11. Vailant, F., Pavageau, E.-M., Bouchcourt, M., Boursier, J.-M. and Lemaire, P., "Modeling the Secondary Side Corrosion of Tubing: A Help to the Maintenance Policy of PWR Steam Generator", *Proc. Of the 9<sup>th</sup> Int. Symp. On Environmental Degradation of Nuclear Mtaerials in Nuclear Power System- Water Reactor*", pp. 679-688, VA, USA, 1999.